has been demonstrated during recent injection studies.[7,8] Pitot rake measurements revealed a spanwise uniform and transversely symmetric Mach 1.98 flow exiting the nozzle section. Nozzle sidewall pressures suggested symmetry of the flow about the spanwise centerline of the tunnel. Finally, total pressure measurements just above the bottom wall illustrated boundary-layer growth.

References

[1]Anon., "ASME Boiler and Pressure Vessel Code B31.1, Section VIII, Unfired Pressure Vessels," American Society of Mechanical Engineers, 1989.

[2]Carroll, B. F., Dutton, J. C., and Addy, A. L., "NOZCS2: A Computer Program for the Design of Continuous Slope Supersonic Nozzles," Univ. of Illinois at Urbana–Champaign, UILU ENG 86-4007, Urbana, IL, 1986.

[3]Burke, A. F., "Turbulent Boundary Layers on Highly Cooled Surfaces at High Mach Numbers," Air Force Aeronautical Systems Div., AFASD TR 61-645, 1961.

[4]Fiore, A. W., Moore, D. G., Murray, D. H., and West, J. E., "Design and Calibration of the ARL Mach 3 High Reynolds Number Facility," Aeronautical Research Labs., TR 75-0012, 1975.

[5]Pope, A., and Goin, K. L., *High Speed Wind Tunnel Testing*, Wiley, New York, 1965.

[6]Gruber, M. R., and Nejad, A. S., "Supersonic Combustion Research Laboratory: Volume 1-Design and Fabrication," U.S. Air Force Wright Lab., WL-TR-93-2052, Wright–Patterson AFB, OH, 1993.

[7]Glawe, D. D., Donbar, J. M., Nejad, A. S., Sekar, B., Samimy, M., and Driscoll, J. F., "Parallel Fuel Injection from the Base of an Extended Strut into Supersonic Flow," AIAA Paper 94-0711, Jan. 1994.

[8]Gruber, M. R., Nejad, A. S., Chen, T. H., and Dutton, J. C., "Mixing and Penetration Studies of Sonic Jets in a Mach 2 Freestream," *Journal of Propulsion and Power*, Vol. 11, No. 2, 1995, pp. 315–323.

Planar Measurement of Absolute OH Concentration Distributions in a Supersonic Combustion Tunnel

T. M. Quagliaroli,* G. Laufer,† R. H. Krauss,‡ and J. C. McDaniel Jr.§
University of Virginia, Charlottesville, Virginia 22903

Introduction

NONINTRUSIVE diagnostic techniques have been shown to provide the necessary spatial resolution and the high measurement accuracy required for the validation of computational codes used to predict mixing and reaction in supersonic combustion facilities. Planar laser-induced fluorescence (PLIF) techniques are particularly suitable for the analysis of both nonreacting[1] and combusting gas flows[2] since they require only modest optical access and can provide the signal-to-noise ratio (SNR) and resolution required for accurate quantitative imaging. PLIF measurements involving molecular species naturally occurring in the flow, such as O_2, OH, and NO, have been used extensively for flow visualization and to determine two-dimensional velocity, temperature, and number density distributions.

OH PLIF has been used in a large variety of applications for measurements of velocity,[3] density, and temperature,[4] in both laminar and turbulent flames. Recently, a new approach for planar laser-induced fluorescence imaging of OH using a KrF excimer laser has been suggested[5] and demonstrated in a supersonic combustion facility.[6]

The objective of the present work was to demonstrate the KrF technique for quantitative PLIF imaging of OH concentration in a model H_2–air scramjet combustor. The fluorescence images were obtained following excitation by a KrF excimer laser operating at 248 nm, resonant with the $^2\Sigma^+(v' = 3) \leftarrow {}^2\Pi(v'' = 0)$ excitation band of OH. Absolute OH density distributions were obtained from the fluorescence images by using, as a reference source, the OH formed in a high-temperature electric furnace.[7] The effect on systematic error induced by collisional quenching by the major species has been assessed.

Theoretical Background

The fluorescence yield following the excitation of the $^2\Sigma^+(v' = 3) \leftarrow {}^2\Pi(v'' = 0)$ band in the A-X system of OH by a KrF laser has previously been evaluated theoretically for a range of temperatures and OH densities.[8] In a typical imaging PLIF experiment the total OH fluorescence in photoelectrons per pixel n_{pe} detected by an electronic camera consisting of an array having $n_p \times m_p$ pixels, increases linearly with its density, N_{OH}, and the relative occupational density of the probed state $\beta(T)$. However, the fluorescence signal is also a function of the spectroscopic properties of OH, as well as laser system and collection optics parameters. The uncertainty in determining these parameters limits the accuracy of the density measurement. Therefore, an independent PLIF measurement of N_{OH} in a calibrated OH source must be used to determine experimentally a calibration coefficient that is representative of system parameter effects and the spectroscopic coefficients.

The use of a high-temperature furnace to produce a stable, easily characterized source of OH for calibration of OH density measurements has recently been reported.[7] The OH fluorescence in this noncombusting environment has been shown[7] to result only from thermal dissociation of H_2O molecules. With known temperature, pressure, and relative humidity, equilibrium OH density in the furnace was calculated using the chemical equilibrium code STANJAN. Equilibrium OH mole fraction in excess of 10^{-4} was obtained. Having this density, direct relation between OH density and LIF quantum yield could be measured, using known laser pulse energy. The measured calibration coefficient accounts for the spectroscopic constants, optical, and geometrical parameters of the measurement, and laser beam parameters such as linewidth or locking efficiency. When the optical and geometrical parameters are identical for both the calibration and experimental measurements, N_{OH} can be determined by directly scaling the experimental photon count per unit laser energy by the predetermined calibration coefficient. A correction for the temperature dependence of $\beta(T)$ may be required, via the Boltzmann distribution. However, selection of an excitation transition with weak temperature dependence may allow for accurate density measurements without a prior temperature measurement.

Presented as Paper 93-0042 at the AIAA 31st Aerospace Sciences Meeting and Exhibit, Reno, NV, Jan. 10–14, 1993; received March 3, 1994; revision received Dec. 9, 1994; accepted for publication Dec. 17, 1994.

*Research Assistant, Aerospace Research Laboratory, Department of Mechanical and Aerospace Engineering, 570 Edgemont Rd. Student Member AIAA.

†Associate Professor, Aerospace Research Laboratory, Department of Mechanical and Aerospace Engineering, 570 Edgemont Rd. Senior Member AIAA.

‡Research Associate Professor, Aerospace Research Laboratory, Department of Mechanical and Aerospace Engineering, 570 Edgemont Rd. Member AIAA.

§Professor, Aerospace Research Laboratory, Department of Mechanical and Aerospace Engineering, 570 Edgemont Rd. Member AIAA.

Experimental Apparatus and Procedure

Planar images of the OH density distributions were obtained in a continuous-flow, electrical-resistance-heated, high-enthalpy, hydrogen–air combustion tunnel.[9] Mach 2 airflow at a stagnation pressure of 287 kPa and stagnation temperature of 1141 K entered the model scramjet combustor consisting of a 2.5 × 3.8 cm constant-area duct, with downstream transverse hydrogen injection behind a rearward-facing, 0.51-cm step. A circular 2-mm injector, providing fuel at a pressure of 378 kPa, temperature of 453 K, and flow rate of 0.54 gm/s, was positioned approximately 3 step heights downstream of the step. Optical access was provided through fused silica windows at the sidewalls, and through an observation window opposite the injector wall.

The illumination and detection configuration is shown in Fig. 1. The OH fluorescence was excited using a narrow-band, tunable KrF laser operating near 248 nm, with a bandwidth of 0.4 cm^{-1}. The wavelength of the laser was tuned using a diffraction grating, positioned by a motorized variable-speed linear actuator with the addition of a piezoelectric linear actuator for fine adjustment. Typical laser energy was ~96 mJ/pulse at the test section, where the beam was shaped into an ~4.6 cm wide by ~0.2 mm thick sheet.

By using a small portion of the laser beam, absorption transitions were selected by detecting the LIF produced in a small propane–air reference flame. The fluorescence produced in the combustor test section following the laser excitation was detected through the observation window by a camera with a 576 × 384 charge-coupled device (CCD) array, uv intensified and gated, and fitted with a uv-clear 105-mm f/4.5 lens. A flowfield volume of ~0.2 × 0.2 × 0.2 mm was imaged by each pixel of the detector array. Filtering was provided by a 10-nm bandpass filter centered at 297 nm and a Schott UG-11 glass filter. This optimized collection of the $^2\Sigma^+(v' = 3) \rightarrow {}^2\Pi(v'' = 2)$ emission band of OH while rejecting radiation due to chemical luminescence and scattered laser light.

Correction for spatial variation in the laser sheet intensity was achieved by splitting a small portion of the sheet just after the final collimating lens (see Fig. 1). This split portion was projected onto a screen and imaged by a second CCD camera. The recorded image was then numerically collapsed to a one-dimensional data field, representing time-averaged spatial intensity variations along the transverse dimension of the sheet. This data field was spatially correlated to the fluorescence image by two registration marks located near the edges of the laser sheet. The overall intensity variation was found to vary $\leq \pm 5\%$ across the sheet, with the largest variation occurring at the edges.

Images of OH fluorescence in the supersonic combustor were obtained in planes parallel to the injector wall. The imaged area spanned a distance from approximately 1 step height upstream of the injector to approximately 8 step heights downstream of the injector. Both the camera and the sheet-forming optics were mounted on precision translation stages. This permitted recording of sequential images at planes parallel to the injection wall, separated by 1 mm.

At each spatial position, two intensity distributions were recorded, each representing an average of 200 laser pulses, normalized by sheet intensity. The first image was obtained with the laser tuned to the absorption transition. A second image was obtained with the laser tuned off resonance. Subtraction of the second from the first provided the background correction for any radiation not originating from the desired narrow-band excitation. When recording the background images the fluorescence output from the small propane flame was monitored to avoid tuning the laser to regions where O_2 excitation would occur and to verify that the amount of detuning from the absorption line center was reproduced at each imaging position.

The OH source used for the calibration was an electrical-resistance heated atmospheric furnace capable of operating at temperatures of up to 1875 K,[7] designed for optical access through three walls. Internal furnace temperature was monitored by two thermocouples with a specified 0.5% uncertainty. Since the furnace was exposed to the atmosphere, internal atmospheric conditions could be determined by monitoring external conditions and furnace temperature. Ambient humidity and atmospheric pressure were measured using a psychrometer and a standard mercury barometer, respectively.

Both the OH calibration images and the combustion tunnel images were obtained using the same detection system, with

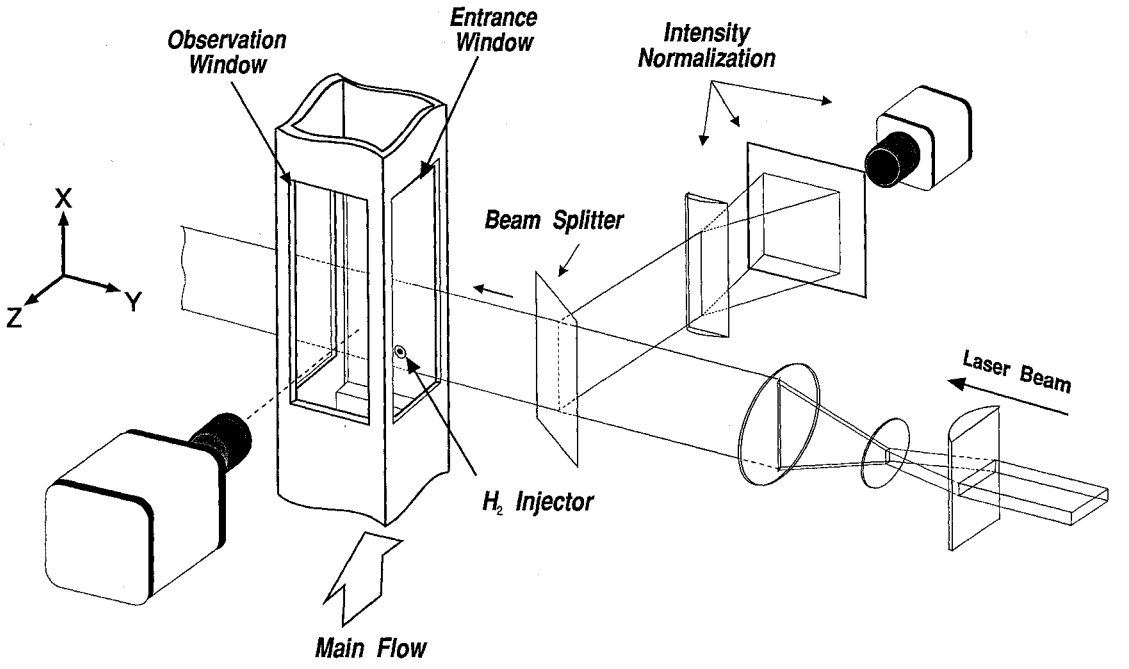

Fig. 1 Experimental configuration for the imaging of OH density distributions. Preheated air enters the duct from below. H_2 is injected by a single injector behind a rear-facing step.

the exception of the collection solid angles, which were measured separately. Thus, the relationship between the measured signal and OH concentration, established by calibration, could be extended to permit determination of absolute OH concentration from fluorescence in the supersonic combustion tests.

Results and Discussion

Density measurements using the excitation of a single rotational level and without temperature correction for $\beta(T)$, require that the population density of this level exhibit small variation over the anticipated temperature range and that interfering fluorescence from other species be small. The $Q_2(11)$ absorption transition was selected for imaging the density distribution of OH in the supersonic combustion facility. The population density of the $N = 11$ level increases by approximately 30% as the temperature increases from the lowest temperature limit of 1500 K to an upper limit of 2500 K. Although other OH transitions present lower temperature sensitivities to temperature, the present transition was selected because it offered a high degree of discrimination between OH and background O_2 fluorescence. While interference by O_2 in a combustion environment is expected to be small, it could not be neglected in the calibration furnace where the concentration of OH relative to O_2 is $\leq 0.1\%$. Thus, the choice of a noninterfering transition is more constraining in the calibration furnace. Use of the $Q_2(11)$ transition permits reliable background subtraction in both the calibration and density measurement experiments.

Figure 2 presents contours of the measured OH density distributions obtained in three planes at distances of $Z/H = -0.8$, 0.0, and 0.8, where H is the step height. In these images, the main flow of preheated air is from bottom to top, with the hydrogen injected normal to the page. In the images, the injector is located at $X/H = 0$ and $Y/H = 0$. Each image consists of a 200-pulse average, normalized with laser intensity distribution after the background fluorescence has been subtracted. Single-pulse images were also obtained; however, the images exhibited significant scatter due to both shot noise and turbulent fluctuations.

The values of N_{OH} in each image were obtained by multiplying the signal at each pixel (after correction for background and laser intensity distribution) by the calibration constant. To partially correct for the temperature dependence of $\beta(T)$, the images were also multiplied by the Boltzmann fraction of the $N = 11$ ground state at 1800 K. At 1800 K the calculated Boltzmann fraction represented the average of Boltzmann fractions over the predicted[10] temperature range of 1500–2500 K. The measured OH concentrations are seen to vary from approximately 2.5×10^{15} cm^{-3} in the regions around the injected fuel, to peak values of 2.6×10^{16} cm^{-3}.

A slight asymmetry in the OH density distribution can be observed in Fig. 2. A similar asymmetry was also observed in chemiluminescence images obtained by removing the bandpass filter, blocking the laser beam, and increasing the exposure time. This asymmetry was, therefore, attributed to nonuniformities in the flow, rather than beam absorption or fluorescence-trapping effects.

The overall accuracy of the measurements is limited primarily by the variation of the $N = 11$ population over the temperature range. At a fixed temperature of 1800 K, for which $\beta(T)$ was evaluated, an uncertainty of $\pm 15\%$ is anticipated. The calibration measurement is expected to contribute a 6% uncertainty, due to a wet-bulb temperature measurement uncertainty of 1 K. The combined uncertainty is 21%. Reduction in the uncertainty of this density measurement could be provided by an independent local OH temperature measurement. The effects of quenching by H_2O, the strongest electronic quenching species,[11] have been considered. The largest H_2O concentration in nonvitiated flows is obtained in a near stoichiometric, $\Phi = 1.0$, atmospheric H_2–air flame. Using published quenching cross sections,[12] the electronic quenching rate by H_2O is expected to be $k_Q \cong 4.5 \times 10^8$ s^{-1}, for a pressure of 1 atm and a temperature of 2000 K. For comparison, the predissociation rate[13] of the $v' = 3$, $J' = 11.5$ level is $k_{pre} = 1.33 \times 10^{10}$ s^{-1}. Therefore, during the lifetime of the excited state, less than 5% of the population is electronically quenched by H_2O.

Quenching by vibrational energy transfer (VET) due to other major species, most importantly N_2 (Ref. 14), has been shown to cause ~1% loss[15] of the initially excited molecules in the $v' = 3$ state in atmospheric flames. However, similar VET quenching in the calibration furnace offsets matching error induced by N_2 quenching in the flame. Therefore, the total additional error introduced due to collisional quenching would be ~5%.

Although the error associated with collisional quenching may increase in regions following shock waves, the present test was run at near thermal choking conditions. Shocks pres-

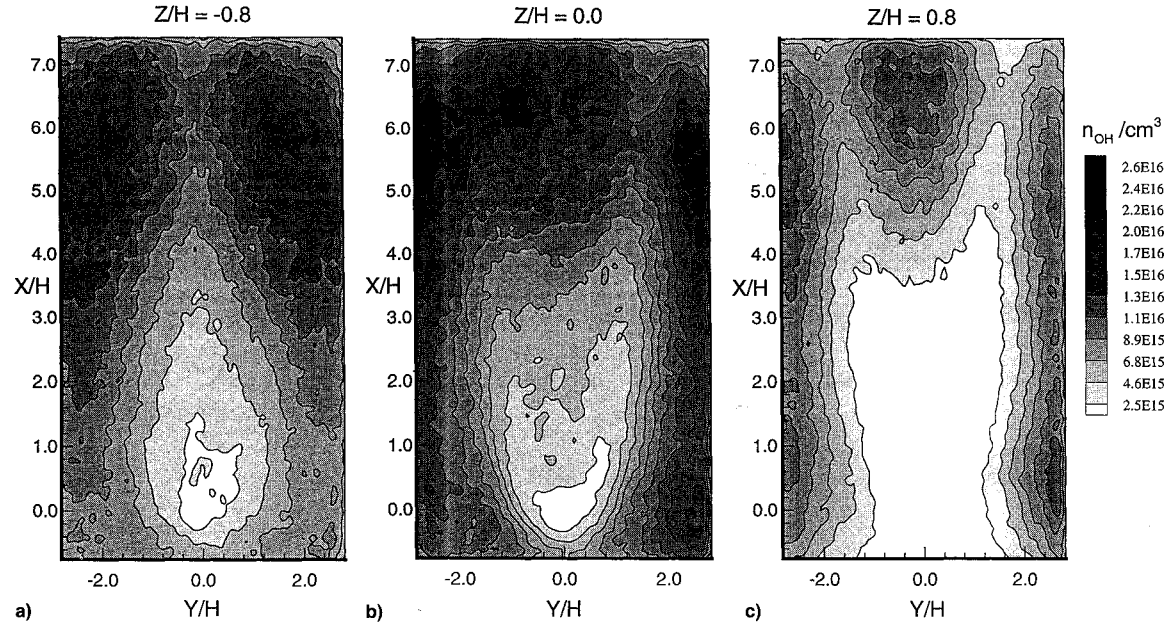

Fig. 2 Measured OH concentrations in planes normal to the injector axis at normalized distances of Z/H = a) −0.8, b) 0.0, and c) 0.8.

ent in the flame region had to be weak and were imperceptible in the fluorescence images.

Conclusions

Planar LIF images of OH in a supersonic combustion test section were obtained by the excitation of the $Q_2(11)$ rovibronic transition. OH densities were obtained from these images by calibration with an OH source generated by the thermal dissociation of H_2O in an atmospheric air furnace. Peak OH concentrations of 2.6×10^{16} cm^{-3} were measured with a predicted uncertainty of ~21%.

Acknowledgments

The work was supported by the NASA Graduate Student Research Program Contract NGT-S0714, and by NASA Grant NAG-1-795, G. Burton Northam, Technical Monitor. The authors acknowledge the considerable contributions made by Jay Grinstead and Steven Hollo.

References

[1]McDaniel, J., Fletcher, D., Hartfield, R., Jr., and Hollo, S., "Staged Transverse Injection into Mach 2 Flow Behind a Rearward-Facing Step: A 3-D Compressive Test Case for Hypersonic Combustor Code Validation," AIAA Paper 91-5071, Dec. 1991.

[2]Grieser, D. R., and Barnes, R. H., "Nitric Oxide Measurements in a Flame by Laser Fluorescence," *Applied Optics*, Vol. 19, No. 5, 1980, pp. 741–743.

[3]Klavuhn, K. G., Gauba, G., and McDaniel, J. C., Jr., "High Resolution OH LIF Velocity Measurement Technique for High-Speed Reacting Flows," AIAA Paper 92-3422, July 1992.

[4]Allen, M. G., Parker, T. E., Reinecke, W. G., and Legner, H. H., "Instantaneous Temperature and Concentration Imaging in Supersonic Air Flow Behind a Rear-Facing Step with Hydrogen Injection," AIAA Paper 92-0137, Jan. 1992.

[5]Andresen, P., Bath, A., Gröger, W., Lülf, H. W., Meijer, G., and Ter Meulen, J. J., "Laser-Induced Fluorescence with Tunable Excimer Lasers as a Possible Method for Instantaneous Temperature Field Measurements at High Pressures: Checks with an Atmospheric Flame," *Applied Optics*, Vol. 27, No. 2, 1988, pp. 365–378.

[6]Quagliaroli, T. M., Laufer, G., Hollo, S. D., Krauss, R. H., Whitehurst, R. B., III, and McDaniel, J. C., Jr., "KrF Laser-Induced OH Fluorescence Imaging in a Supersonic Combustion Tunnel," *Journal of Propulsion and Power*, Vol. 10, No. 3, 1994, pp. 377–381.

[7]Grinstead, J. H., Laufer, G., and Krauss, R. H., "A Calibration Source for OH Laser-Induced Fluorescence Density Measurements Using Thermally Dissociated H_2O in Atmospheric Air," *Applied Optics*, Vol. 33, No. 6, 1994, pp. 1115–1119.

[8]Quagliaroli, T. M., Laufer, G., Krauss, R. H., and McDaniel, J. C., Jr., "Evaluation of OH Laser-Induced Fluorescence Techniques for Supersonic Combustion Diagnostics," *AIAA Journal*, Vol. 31, No. 3, 1993, pp. 520–527.

[9]Krauss, R. H., and McDaniel, J. C., Jr., "A Clean Air Continuous Flow Propulsion Facility," AIAA Paper 92-3912, July 1992.

[10]Segal, C., "Experimental and Numerical Investigation of Hydrogen Combustion in a Supersonic Flow," Ph.D. Dissertation, Univ. of Virginia, Charlottesville, VA, Aug. 1991.

[11]Kohse-Höinghaus, K., Jeffries, J. B., Copeland, R. A., Smith, G. P., and Crosley, D. R., "The Quantitative LIF Determination of OH Concentrations in Low-Pressure Flames," *Twenty-Second Symposium (International) on Combustion*, The Combustion Inst., Pittsburgh, PA, 1988, pp. 1857–1866.

[12]Barlow, R. S., Dibble, R. W., and Lucht, R. P., "Simultaneous Measurement of Raman Scattering and Laser-Induced OH Fluorescence in Nonpremixed Turbulent Jet Flames," *Optics Letters*, Vol. 14, No. 5, 1989, pp. 263–265.

[13]Heard, D. E., Crosley, D. R., Jeffries, J. B., Smith, G. P., and Hirano, A., "Rotational Level Dependence of Predissociation in the $v' = 3$ Level of OH $A^2\Sigma^+$," *Journal of Chemical Physics*, Vol. 96, No. 6, 1992, pp. 4366–4371.

[14]Copeland, R. A., Wise, M. L., and Crosley, D. R., "Vibrational Energy Transfer and Quenching of OH($A^2\Sigma^+$, $v' = 1$)," *Journal of Chemical Physics*, Vol. 92, No. 20, 1988, pp. 5710–5717.

[15]Steffens, K. L., Jeffries, J. B., and Crosley, D. R., "Collisional Energy Transfer in Predissociative OH Laser-Induced Fluorescence in Flames," *Optics Letters*, Vol. 18, No. 16, 1993, pp. 1355–1357.

New Stabilizers for Double-Base Propellants

Adly A.-W. Soliman,* A. A. El-Damaty,† and M. A. M. Hassan‡
National Institute for Standards, El Harram, Giza, Egypt

I. Introduction

A NUMBER of malondianilide derivatives have been used in a wide range of industrial applications,[1–5] in other different fields,[6–10] and in continuation of our previous work.[11–13] We have investigated *N,N*-diphenylmalondianilide derivatives (1*a*, *b*) to use them as stabilizers for double-base propellants, to examine the explosive properties of the malondianilide molecule, and to study another type of application of these compounds. The compounds prepared as indicated in previous literature[14–16] and the structural assignment have been proved by elemental analysis and IR spectrum:

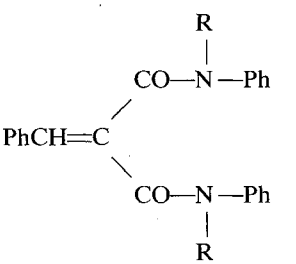

1*a*, R = H
b, R = C_2H_5

II. Experimental

The sample mixtures, which contain nitrocellulose (12.10% N) 56%, nitroglycerin 27%, dinitrotoluene 9%, dibutylphthalate 4%, dianilide compound 3%, and transformer oil 1%, are treated according to the different steps used in production of double-base propellant.

The stability tests,[17] the calorific test carried out on the samples, and the results are tabulated in Table 1. The tests of calorific value prove that the compound (1*b*) has an endothermic action and ranged between −25 cal/g to −33 cal/g (average −29 cal/g). The comparison was carried out between centralite 1 sample (diethyldiphenylurea, 22.6 cal/g) and stabilizer 1*b* sample.

The results of the stability tests shown in Table 1 indicate that the dianilides have a distinct stabilizing effect in double-base propellant. This fact was clearly confirmed by the calculation of the half lifetime of sample III in comparison with sample I as a stabilizer. Storage tests at 100, 90, and 80°C were done under the same conditions and weight of the samples.[18] The rest of the stabilizer was calculated periodically as shown in Table 2 by using column partition chromatography after the samples were extracted by using different solvents.

The rest of the stabilizers before and after storage for different times are shown in Table 3. The needed time to use 50% of the original stabilizer (sample I = 1.43 and sample III = 1.45%) at different temperatures is tabulated in Table 4.

Received Oct. 19, 1992; revision received Feb. 3, 1993; accepted for publication April 2, 1993.

*Professor, Safety Tests Division.
†Assistant Professor, Safety Tests Division.
‡Safety Tests Division.